

A Discrete Non-Linear Series Elastic Actuator for Active Ankle-Foot Orthoses

Benjamin DeBoer¹, Ali Hosseini¹, and Carlos Rossa²

Abstract—This letter outlines the modelling, design, and experimental validation of a novel power-efficient actuator for an active ankle-foot orthosis (AAFO). The actuator is based on a new principle of discrete non-linear stiffness. Two or more linear springs are discretely compressed at specified displacement intervals to reduce the peak mechanical power required to actuate the AAFO. The actuator uses a crank-rocker configuration. The connecting link is comprised of the discrete non-linear technique, a DC motor powers the crank, and the rocker is connected directly to the ankle joint. Multi-objective optimization is carried out to select the link lengths and spring stiffnesses to reduce input power and size. The actuator design weighs 460 g with bounding box dimensions of 103x45x94 mm. The newly proposed discrete non-linear stiffness configuration reduces the peak mechanical input power by 77.2% with respect to nominal biological ankle joint power.

A prototype was developed and tested using static loading and human walking trials to verify the actuator models and simulations. The experimental results confirm the validity of the models by comparing the actual and theoretical ankle and motor torque values in the presence of discrete variable stiffness.

Index Terms—Prosthetics and Exoskeletons, Actuation and Joint Mechanisms, Mechanism Design, Rehabilitation Robotics.

I. INTRODUCTION

FOOT drop is a result of stroke or other events that affect the dorsiflexion capability of the ankle joint [1]. The limited dorsiflexion causes the toe to contact the ground during the swing phase and slap the ground during the swing to stance phase, leading to unnatural walking patterns known as steppage and circumduction gait [2].

An ankle-foot orthosis (AFO) is a device that assists patients with dorsiflexion and plantarflexion difficulties, including foot drop [3]. A passive AFO is composed of a shank, footbed, and hinging element. Passive devices restrict the plantarflexion motion of the foot to eliminate toe contact and foot slap; however, an altered gait is required to maintain adequate clearance between the foot and the ground. Active AFOs (AAFO) is the evolution of passive AFOs. The goal is to assist a patient in achieving a natural gait cycle by applying torque to the ankle joint, causing the foot to dorsiflex and plantarflex.

A natural gait for a 80.5 kg user with a 1.1 s gait time requires a peak biological power of 263 W at the ankle joint [4]. Therefore, direct-drive AAFO actuation systems

would be bulky and impractical. Thus, alternative actuation methods have been proposed to reduce the peak power input. The design of compliant and power-efficient actuators for an AAFO closely resembles those found in active ankle-foot prostheses. Current actuator designs employ the well-known series elastic actuator (SEA) concept and its evolution to the variable stiffness actuator (VSA).

SEAs generate torque at the ankle joint via a DC motor and compliant link. In a SEA, the displacement of a compliant link (most commonly a non-linear or linear spring) can be measured to infer the applied force/torque based on the compliant link and lever arm characteristics. The goal of the SEA in AAFOs is first to add compliance between the user and control device. However, the configuration has been successfully used for regenerative braking. Some examples of SEA configurations in AAFOs include the robotic tendon developed by Hollander *et al.*, with a design capable of reducing the peak input power of an AAFO by 69% compared to the direct-drive alternative; optimizing the stiffness of a linear spring placed between a slider and crank [5]. The energy applied by the motor and absorbed from the ankle joint is stored in the spring until it is required, termed regenerative braking [6]. The design is capable of outputting 50% of the ankle joint power for a 65 kg user, with a mass of 0.5 kg [7]. Convens *et al.* developed an actuator that combines a resettable overrunning clutch with a series elastic actuator, allowing the load to be removed from the motor and energy to be stored in a spring during the stance phase, reducing the peak power and energy requirements of the driving motor [8]. Extensive research has been conducted on the implementation of parallel elastic actuators (PEA), SEA, and their combination to reduce peak input power and energy, reducing the peak mechanical input power by 70% using a SEA and PEA combination [9]. Peak input power reduction is still the main focus of actuator design as of recent. Work by Liu *et al.*, showed that the implementation of a unidirectional parallel spring will reduce the peak input power by 74.3% compared to the direct-drive alternative, with an additional 0.08% peak power reduction when combined with a SEA [10].

VSAs are designed to enable stiffness variation of an actuator to best suit the required output force/torque requirements. These configurations are mechanically complex compared to the original SEA, in which many links, rotating disks, and springs are employed. An example is an actuator presented in [11] where a linear spring generates a torque based on the difference between two links, one of which is driven and the other is attached to the ankle joint. The design produces 25 Nm of torque with a total weight of 1.7 kg. Another example

¹Benjamin DeBoer and Ali Hosseini are with Faculty of Engineering and Applied Science, Ontario Tech University, Oshawa, Ontario, Canada. benjamin.deboer1@ontariotechu.net, SayyedAli.Hosseini@ontariotechu.ca

²Carlos Rossa is with Department of Systems and Computer Engineering, Carleton University, Ottawa, Ontario, Canada. rossa@sce.carleton.ca
Digital Object Identifier (DOI): see top of this page.

is a barrel-based VSA for unpowered ankle exoskeletons, in which tensile springs are mounted between a fixed (bottom) and rotating (top) plate. The stiffness decreases as the top plate rotation increases [12]. The authors in [13] propose a design that modulates the ankle joint stiffness for accurate control from the swing phase to toe contact. The rotation of a cam shifts the pivot point to increase or decrease the distance between the pivot, spring, and output point, thereby generating a varying stiffness.

In the presented SEA and VSA designs, varying linkage configurations are employed to apply the assistive torque, commonly using a four-bar mechanism in a slider-crank configuration [7]. An inherent advantage of the crank-rocker four-bar mechanism is that the torque of the motor is reduced to zero when the driven and connecting links are aligned [14]. These arrangements allow the AAFO to be optimized in terms of tracking error, mass, peak power, or energy consumption.

While the actuators mentioned above provide significant power reduction with a SEA and stiffness variation with the VSA, the ideal combination of each actuator's benefits has not been thoroughly explored. The goal of an AAFO actuator is to have the capability to apply full power assistance when required while minimizing the mass of the device. In ankle-foot prosthesis design, the mass of a prosthesis can be designed to match the mass of the amputated limb, and thus the more complex above-mentioned actuators can be employed. In the case of AAFOs, the user's lower limbs are present, resulting in a significant increase in the metabolic cost of walking due to the external mass [8]. Therefore, the objective of the AAFO actuator design must be focused on mass minimization while still providing the required assistance. The objective can be reached by minimizing the size and complexity of the actuator design while reducing the peak required power. Consequently, reducing the size of the driving motor and related electronics. The implemented linkage configuration can also be further explored to aid the above objective, utilizing the inherent mechanical advantage of alternative four-bar mechanisms as initially identified by [14].

The present paper proposes a compact low-power actuator for an AAFO, combining the methods of variable stiffness with the input power reduction capability of the optimized SEA and unidirectional PEA. The device combines a crank-rocker mechanism with a discrete non-linear compliant link to create a VSA. A crank-rocker configuration is employed to reduce the holding torque required during high biological ankle power instances within the gait. The discrete non-linear method is conceptualized and implemented to occupy a low footprint while minimizing the mechanical power required by the driving motor. The discrete non-linear method is simple: a set of linear springs are engaged at discrete displacement intervals to generate the optimal trade-off between power consumption and actuator mass. The combination of the discrete non-linear SEA and crank-rocker configuration results in a peak mechanical power reduction of 77.2% with respect to the nominal biological ankle power. The model and simulations are validated using an AAFO prototype encompassing the presented actuator (See Fig. 1).

This paper is structured as follows: Section II describes

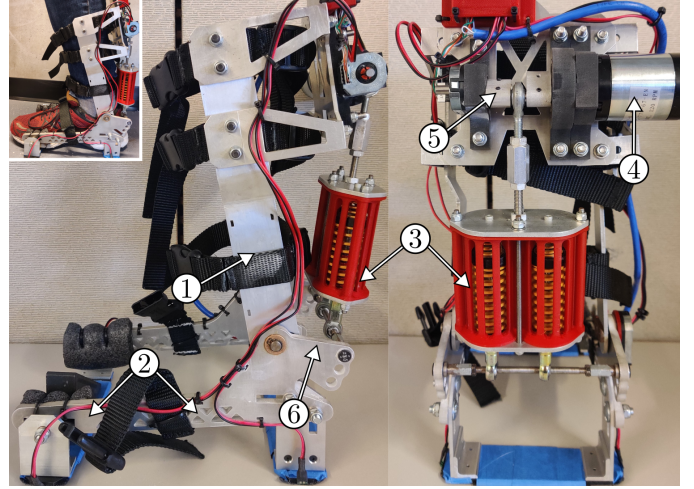


Fig. 1. Constructed AAFO prototype with a peak power output of 174.1 W at the ankle joint with a total weight of 2.85 kg. ① Shank, to be attached to the users leg, ② is the foot-bed to house the users foot. ③ is the constructed discrete non-linear SEA. ④, ⑤, and ⑥ are the DC motor and gearbox, crank, and rocker linkages, respectively.

the novel discrete non-linear crank-rocker theory, section III optimizes the proposed actuator and section IV compares it to the equivalent linear SEA, section V outlines the prototype and physical tests conducted to validate the actuator, and VI concludes and lays out the road map for future works.

II. DISCRETE NON-LINEAR STIFFNESS

The actuator proposed in this paper replaces the linear compliant link of a SEA with a discrete non-linear compliant link. The method engages linear springs at discrete instances of the gait cycle, based on the required assistive torque. The discrete non-linear spring rate is evaluated in a crank-rocker configuration, as shown in Fig. 2(b). The crank (a) is the driving link, connected to the driven link (c) by the discrete non-linear link b . The discrete non-linear method (see Fig. 2(a)) is based on the engagement of a set number (n) of linear spring at set displacements ($\delta_{Off_2}, \dots, \delta_{Off_n}$), resulting in a discrete change in actuator stiffness. The acting spring rate of link b can be determined by:

$$k = \begin{cases} k_1, & \text{if } \delta_b < \delta_{Off_2} \\ k_1 + k_2, & \text{if } \delta_b < \delta_{Off_3} \\ \vdots & \vdots \\ \sum_{i=1}^n k_i, & \text{Otherwise} \end{cases} \quad (1)$$

where δ_b is the extension/compression of link b , and δ_{Off_n} is the displacement in which spring n engages. k_1, \dots, k_n are the primary and discrete spring stiffness where k_1 is always engaged and k_2 to k_n are unidirectional series springs. The method of discrete stiffness allows the application of one or multiple unidirectional series springs to generate an approximation of the non-linear stiffness required for optimal regenerative braking at the ankle joint.

The ankle position and torque of a nominal gait cycle is known [4], therefore, the input power required by the driving

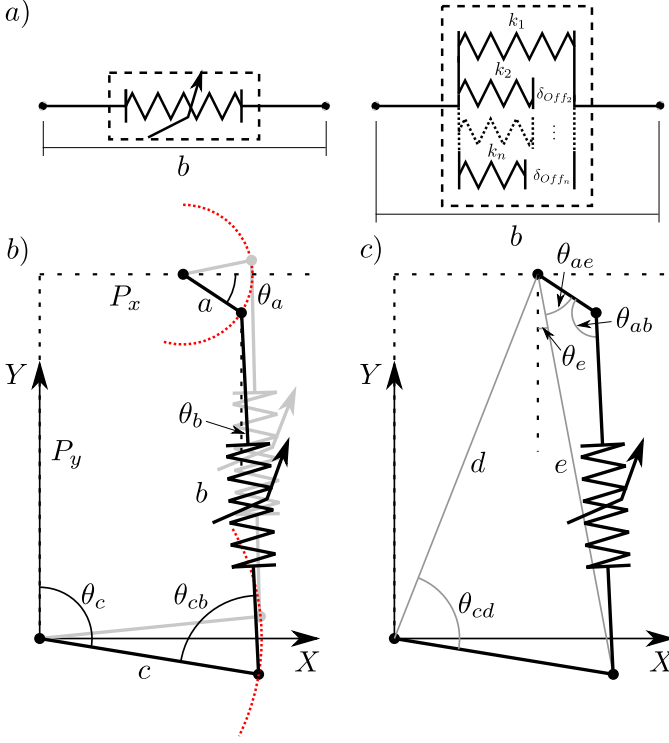


Fig. 2. a) The discrete non-linear compliant link, in which the link has the stiffness k_1 until the displacement δ_{Off_2} is reached and $k_1 + k_2$ until δ_{Off_3} is achieved, in which the stiffness has another discrete change. b) Crank-rocker actuator in which link a is driven by a motor and gearbox combination, link b is the discrete non-linear link shown in 2(a), and link c pivots about the ankles axis of rotation to provide rotation (θ_c) and torque (τ_c). c) Additional trigonometric angles and lengths required to solve the discrete non-linear crank-rocker equations.

motor to achieve the nominal gait can be determined and minimized. To identify the optimal spring stiffnesses and discrete activation displacements, the kinematics of the crank-rocker designs (Fig. 2) must be evaluated.

The crank-rocker mechanism has an inherent structure that reduces the holding torque required by the motor when links a and b are parallel. The mechanism (See Fig. 2(b)) is driven by the rotation of link a with the advantage of the required torque at link a (τ_a) in reference to the force within link b (F_b), having the relationship:

$$\tau_a = F_b \cdot a \cos(\theta_a - \theta_b) \quad (2)$$

When links a and b are parallel $\tau_a = 0$. Therefore, to solve the angular position and torque at link a , the length and force within link b are evaluated as:

$$b = b_0 + \Delta b \quad (3)$$

with

$$\Delta b \begin{cases} \frac{F_b - F_{Limit}(0)}{\sum_{j=1}^1 [k_j]}, & \text{If } F_b < F_{Limit}(1) \\ \delta_{Off_2} + \frac{F_b - F_{Limit}(1)}{\sum_{j=1}^2 [k_j]}, & \text{If } F_b < F_{Limit}(2) \\ \vdots & \vdots \\ \delta_{Off_n} + \frac{F_b - F_{Limit}(n-1)}{\sum_{j=1}^n [k_j]}, & \text{If } F_b < F_{Limit}(n) \end{cases} \quad (4)$$

governed by:

$$F_{Limit}(n) = \sum_{i=1}^n \left[\sum_{j=1}^i [k_j] (\delta_{Off_{i+1}} - \delta_{Off_i}) \right] \quad (5)$$

where b_0 is the initial length of link b . F_b is dependent on the angle of links c (θ_c) and b (θ_b) and torque applied at the ankle joint (τ_c) calculated as:

$$F_b = \frac{\tau_c}{c \sin(\theta_c - \theta_b)} \quad (6)$$

To solve for the position of link a (θ_a), see Fig. 2(c), a set of trigonometric functions are required. The length d in Fig. 2(c) is:

$$d = \sqrt{P_X^2 + P_Y^2} \quad (7)$$

and the angle θ_{cd} between length d and c is:

$$\theta_{cd} = \theta_c - \arctan\left(\frac{P_X}{P_Y}\right) \quad (8)$$

Leading to the distance between the end of link c and the rotation point of link a :

$$e = \sqrt{c^2 + d^2 - 2cd \cos(\theta_{cd})} \quad (9)$$

The angle between length e and negative Y axis:

$$\theta_e = \arctan\left(\frac{P_{Cx} - P_X}{P_{Cy} + P_Y}\right) \quad (10)$$

in (10):

$$P_{Cx} = c \cos \theta_c, \quad P_{Cy} = c \sin \theta_c$$

Furthermore, the angle between length e and link a is:

$$\theta_{ae} = \arccos\left(\frac{e^2 + a^2 - b^2}{2ae}\right) \quad (11)$$

Finally, θ_a is calculated as:

$$\theta_a = \theta_{ae} + \theta_e - \frac{\pi}{2} \quad (12)$$

and the value of θ_b can then be determined by:

$$\theta_b = \arctan\left(\frac{c \sin \theta_c - P_X - a \cos \theta_a}{c \cos \theta_c - a \sin \theta_a + P_Y}\right). \quad (13)$$

Since F_b (6) is dependent on θ_b (13) and θ_b is dependent on F_b an iterative approach is required to find position θ_a . Therefore, to start the iterations $\theta_b = 0$ and Eqns, (3), (6), and (11 - 13) are iterated until a set error threshold of θ_b is reached. The position of θ_b is iterated as follows:

$$\theta_b(i+1) = \underbrace{\gamma(\theta_b(i) - \theta_b(i-1))}_{\text{Error}} + \theta_b(i-1) \quad (14)$$

where $\gamma > 0$ is a scalar gain. Once the final position of θ_a is calculated for each instance of the known ankle angular and torque trajectory, the power required by the motor driving the crank-rocker actuator is determined as:

$$P = \frac{d\theta_a}{dt} \tau_a \quad (15)$$

Fig. 3, demonstrates the ability of the discrete non-linear method with one discrete stiffness change ($n = 2$) to reduce the peak input power to the system. A 24.3% peak power

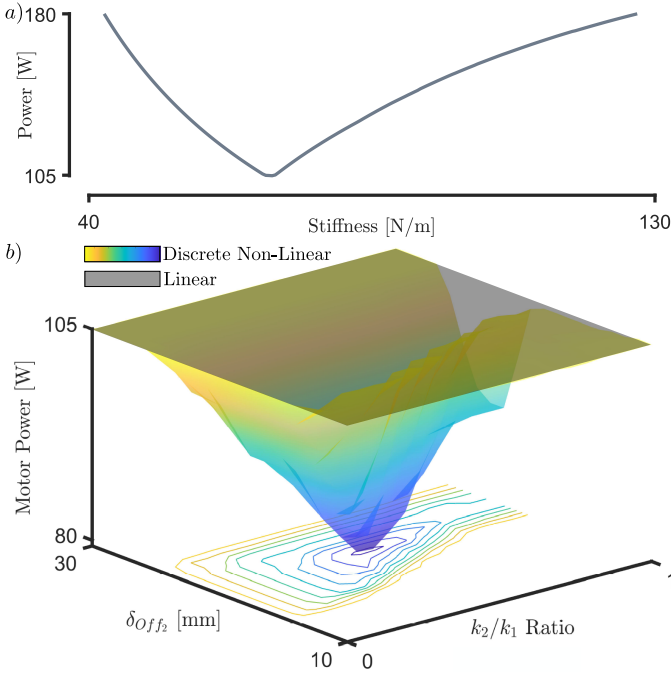


Fig. 3. Peak mechanical power based on a range of stiffness for a linear (a) and discrete non-linear (b) SEA. The test is conducted on a crank-rocker actuator with the following fixed parameters: $b_0 = 200$ mm, $c = 60$ mm, and $P_X = 60$ mm. a) Minimum linear power output for a range of k . b) Minimum discrete non-linear ($n = 2$) power output for a range of k_2/k_1 and activation offset values δ_{off_2} (See Fig. 2(a)), when spring rate k_1 is iterated from 1 N/mm to 150 N/mm and the minimal power is plotted for each instance. The grey plan represents the minimum power output from the above linear simulation (a).

reduction is seen by the discrete non-linear design compared to the linear design. Optimization of the actuator configuration is completed to further exploit the benefits of the discrete non-linear design and crank-rocker topology.

III. ACTUATOR OPTIMIZATION

To find the best design for the discrete non-linear actuator described in Sec. II with $n = 2$, optimization of the various link lengths, offsets, and spring stiffnesses is done. Non-dominated Sorting Genetic Algorithm II (NSGA-II) [15] is employed to minimize the peak power and total length of two actuator configurations:

1. Discrete non-linear crank-rocker
2. Linear crank-rocker (as in $n = 1$)

The decision variables are as follows, $[P_X, P_Y, a, b_0, c, k_1, k_2, \delta_{off_2}, \theta_{adj}]$ where θ_{adj} is an angular offset of θ_c . The objective of the optimization is to minimize the mechanical input power to the device, while minimizing the overall length of the employed linkage configuration, defined as:

$$\text{Minimize: } \begin{cases} P_{max} = \max(|P|) \\ L = a + b + c + d \end{cases} \quad (15)$$

to target the reduction in mass of the actuator while providing the necessary power to the ankle joint. Minimizing the peak power required at link a results in a smaller (and thus lighter)

motor and gearbox combination. Minimization of the link length limits the size and mass of the linkages.

The optimization of the crank-rocker mechanism is subject to the constraints of trajectory tracking compliance of a nominal gait, as link a limits the displacement range of b . Therefore, if the desired response at θ_c is not achieved, then the values of the minimization objective functions are divided by the penalty scalar $P_s \in [0, 1]$, determined as:

$$P_s = \begin{cases} P_s = 1, & \text{if } valid = 1 \\ P_s = valid \cdot \alpha, & \text{otherwise} \end{cases} \quad (16)$$

with:

$$valid = \frac{|\theta_c| - |\theta_{c-invalid}|}{|\theta_c|} \quad (17)$$

where $\alpha \in [0, 1]$. A population of the selected actuator configuration is randomly generated within a set decision variable range to conduct the optimization. Any population member that results in $P_s < 1$ is discarded. Each iteration of NSGA-II is conducted by solving for link a position (θ_a) and torque (τ_a) for a complete gait cycle. The objective function L is calculated and P_{max} is determined from (15).

To determine a feasible design with market available springs, optimization can be conducted in three steps. The first step is to fix the length of b_0 to allow sufficient room for the spring assembly. The simulation is conducted and the optimized value of k_1 for power reduction is reviewed, and a spring with the closest stiffness and displacement larger than of that required of k_1 is selected. Step two re-conducts the simulation with a fixed value of k_1 identified in the previous step, in which the same selection process is used for k_2 . The final step has fixed values for k_1 , k_2 , and b_0 , in which the final link lengths and offsets are acquired. A complete simulation of the designs is recorded, including the displacement and force within link b , to study each design's energy storage and power application instances.

IV. OPTIMIZATION RESULTS & DISCUSSION

The power the actuator applies to the ankle joint is a combination of spring and motor power. As seen in [5] the total ankle power is:

$$P = \underbrace{\tau_c \dot{\theta}_c}_{\text{Ankle}} = \underbrace{F_b \dot{b}}_{\text{Spring}} + \underbrace{\tau_a \dot{\theta}_a}_{\text{Motor}} \quad (18)$$

The optimization results can be seen in Fig. 4(a). The discrete non-linear design results in a lower peak motor power for a longer duration than the equivalent linear design (See Fig. 4(b)). The power reduction stems from the early energy storage and late energy dispersion provided by the discrete non-linear design. The energy stored in the springs combines user applied (regenerative braking principle), and motor applied energy. The linear and discrete non-linear crank-rocker mechanism saw a 62.4% and 77.2% power reduction, compared to the peak biological ankle joint power, respectively. The peak power reduction stems from the reduced velocity of the motor (Fig. 4(b)) during instances of high torque and power within the gait cycle. The respective energy consumption for the linear and discrete non-linear cracker-rocker is 23.6 J and 19.3

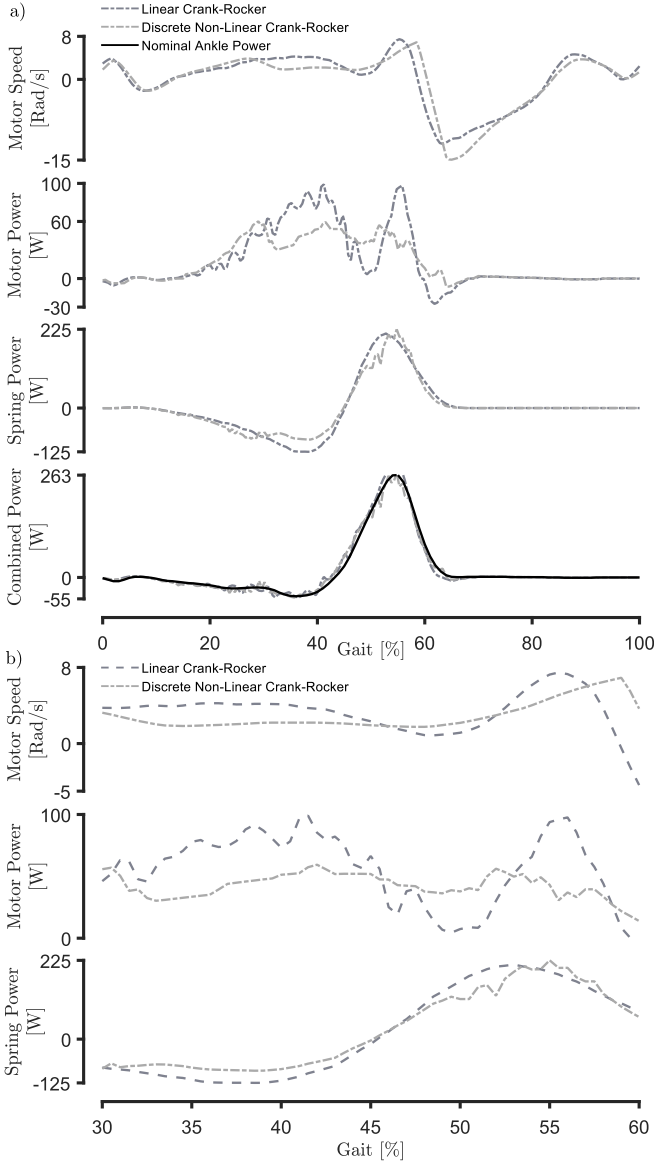


Fig. 4. a) Simulated motor and spring power, matching the required nominal power for a gait cycle. b) A sectioned view of a) (30% - 60%) showing the decrease in power of the discrete non-linear design is attributed to the lower motor velocity at high torque instances.

J, respectively. The results prove the effectiveness of design, reducing the input power by an additional 2.8% compared to the best-presented actuator design in literature [10].

V. EXPERIMENTAL VALIDATION

A prototype is designed and constructed to validate the proposed discrete non-linear design, and the actuator model is verified using a static loading and human walking trial.

A. Actuator Design & Construction

The constructed AAFO prototype (see Fig. 1) is equipped with a discrete non-linear series elastic actuator, with the parameters listed in Table I. The design was optimized using the procedure presented in Sec. III, resulting in a 76% power reduction compared to the nominal biological gait power. The

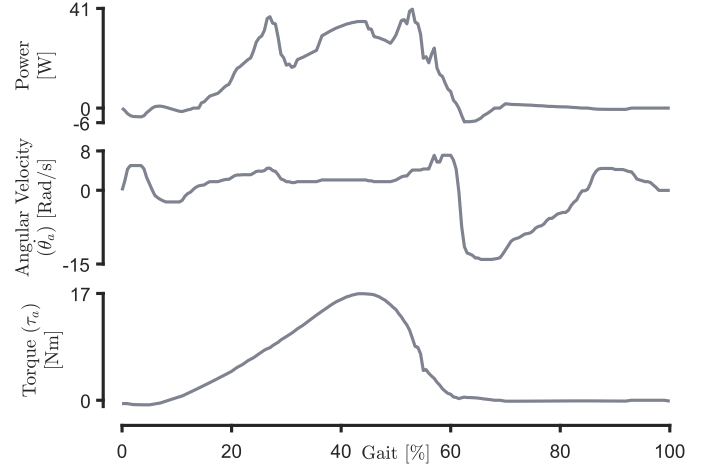


Fig. 5. Motor output for the optimized actuator at 70% maximum torque. The design results outputs a peak power of 174 W at the ankle joint with a peak mechanical input power of 41 W.

TABLE I
OPTIMIZED CRANK-ROCKER DESIGN: FULL ASSISTIVE TORQUE FOR A 56 KG USER.

Parameter	Value	Parameter	Value
P_X	117.83 mm	P_Y	173.78 mm
a	13.49 mm	b	200 mm
c	51.86 mm	θ_{adj}	-0.38 rad
k_1	42.80 N/mm	k_2	51 N/mm
F_{Limit}	739.49 N	δ_{off_2}	17.28 mm

output power, torque, and angular velocity of the motor (link a) are presented in Fig. 5, where the motor torque decreases at high instances of ankle power due to the crank-rocker configuration. The structure of the brace is constructed from aluminum and nylon, with the actuator (See. Fig. 6) comprised of steel springs and connecting rods, aluminum plates, and a PLA enclosure with bounding box dimensions of 103x45x94 mm, weighing 460 g. The control system is designed to track the angular trajectory of the gait cycle, with the desired torque at the ankle joint determined based by tracking error. The desired ankle torque is then translated into the required length of link b , thus determining the required position of the motor. A PD motor position controller is then used to drive the 24V geared DC motor (ES-Motor 150W with a 67 : 1 planetary gearbox) via an H-bridge. Two quadrature encoders are used to measure the position of the motor and ankle joint and a current sensor is implemented to measure the armature current of the DC motor.

B. Actuator Model Verification

In order to verify the actuator model and above formulations, a static loading and human walking trial are conducted. A static loading test allows the accuracy of the applied ankle torque to be determined without human disturbance, followed by a walking trial that verifies the modelled torque of the motor. The output ankle and motor torque of the actuator are determined using the measured rotation of link a and c , by

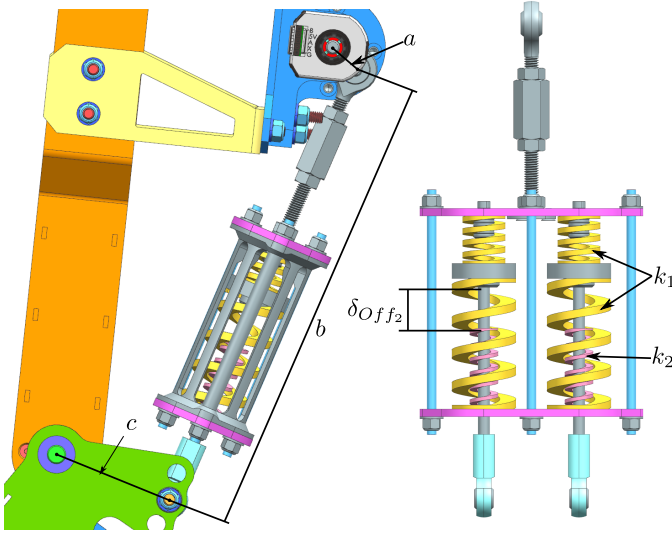


Fig. 6. Constructed discrete non-linear design, in which springs k_1 are applied for both dorsiflexion and plantarflexion compliance. Spring k_2 is applied after a set displacement δ_{Off} as represented in Fig. 2.

analyzing the change in actuator length:

$$\delta b = \sqrt{(P_{Cy} - P_{Ay})^2 + (P_{Cx} - P_{Ax})^2} - b_0 \quad (19)$$

where:

$$P_{Ax} = P_X + a \cos \theta_a, \quad P_{Ay} = P_Y - a \sin \theta_a$$

Results in an axial force in link b , for $n = 2$ of:

$$F_b = \begin{cases} \delta b(k_1), & \delta b < 0 \\ \delta b(k_1), & \delta b < \delta_{Off2} \\ \delta_{Off2}k_1 + (\delta b - \delta_{Off2})(k_1 + k_2), & \text{otherwise} \end{cases} \quad (20)$$

in which the resulting torque at the ankle (τ_c) and motor (τ_a) point of rotation can be expressed as:

$$\tau_a = aF_b \sin(\theta_a + \frac{\pi}{2} - \theta_b); \quad (21)$$

$$\tau_c = cF_b \sin(\theta_c - \theta_b); \quad (22)$$

where θ_b is determined as:

$$\theta_b = \arctan\left(\frac{P_{Ax} - P_{Cx}}{P_{Ay} - P_{Cy}}\right). \quad (23)$$

Both the torque at the ankle and motor joint can be verified with the motor and ankle position and current measurements.

A static loading test is conducted with the AAFO mounted on a rigid test stand. The end of the footbed of the AAFO is placed on a dynamometer (KISTLER Type 9255C) to measure the component reaction force that the AAFO applies to the ground. The length of the lever arm is measured to be 188.5 mm to determine the applied torque by the AAFO. The test required the AAFO to apply torque to the ankle joint in response to a step input. The corresponding modelled torque and measured torque for the experiments are shown in Fig. 7(a). The results prove that the actuator model is accurate. Minor discrepancies in the results can be attributed to the uncertainties in estimating the stiffness constant of the springs.

A human walking trial is also conducted on a clinical treadmill by a user with no gait impairment. The model calculated assistive ankle torques of up to 53 Nm throughout the test. Resulting in the discrete non-linear actuator exceeding the δ_{Off2} displacement multiple times. The torque constant of the motor is inferred from the measured motor current and modelled motor torque to validate the model, as the torque of a motor is directly co-related to the armature current ($\tau = k_i i$). Fig. 7(b) shows the result at instances of high modelled motor torque and current. The signal noise can be linked to the response of the motor position controller. These tests show that the presented model is accurate.

VI. CONCLUSION

This paper presents a novel regenerative braking actuator comprised of a discrete non-linear compliant link. The discrete non-linear actuator can reduce the peak mechanical input power to the system by 77.2% with respect to the nominal biological ankle joint power, a decrease of 2.8% compared to the previous best in literature [10]. The design eliminates the need for lead screws in AAFO actuators, reducing the system's overall size, weight, and complexity. The discrete activation of multiple linear springs requires only one elastic element in the system compared to the SEA and unidirectional PEA, in which two separate elastic elements are required. The downfall of the crank-rocker design is the high non-linearity of the system and the accuracy to which the springs and linkages must comply.

The proposed discrete non-linear actuator proved to be effective in actuating the AAFO. Further development can consider additional ($n > 2$) discrete stages within the actuator to further reduce peak motor power while maximizing the stored energy within the compliant link. While effective, in theory, increasing the number of springs and displacement offsets will significantly increase the actuator's weight.

REFERENCES

- [1] F. D. Westhout, L. S. Paré, and M. E. Linskey, "Central causes of foot drop: rare and underappreciated differential diagnoses," *The journal of spinal cord medicine*, vol. 30, no. 1, pp. 62–66, 2007.
- [2] A. Dubin, "Gait: the role of the ankle and foot in walking," *Medical Clinics*, vol. 98, no. 2, pp. 205–211, 2014.
- [3] Y. J. Choo and M. C. Chang, "Commonly used types and recent development of ankle-foot orthosis: A narrative review," in *Healthcare*, vol. 9, no. 8. Multidisciplinary Digital Publishing Institute, 2021, p. 1046.
- [4] G. Bovi, M. Rabuffetti, P. Mazzoleni *et al.*, "A multiple-task gait analysis approach: kinematic, kinetic and emg reference data for healthy young and adult subjects," *Gait & posture*, vol. 33, no. 1, pp. 6–13, 2011.
- [5] K. W. Hollander, R. Ilg, T. G. Sugar, and D. Herring, "An efficient robotic tendon for gait assistance," 2006.
- [6] A. M. Oymagil, J. K. Hitt, T. Sugar *et al.*, "Control of a regenerative braking powered ankle foot orthosis," in *IEEE International Conference on Rehabilitation Robotics*, 2007, pp. 28–34.
- [7] A. W. Boehler, K. W. Hollander, T. G. Sugar *et al.*, "Design, implementation and test results of a robust control method for a powered ankle foot orthosis (afo)," in *IEEE International Conference on Robotics and Automation*, 2008, pp. 2025–2030.
- [8] B. Convens, D. Dong, R. Furnémont *et al.*, "Modeling, design and test-bench validation of a semi-active propulsive ankle prosthesis with a clutched series elastic actuator," *IEEE Robotics and Automation Letters*, vol. 4, no. 2, pp. 1823–1830, 2019.
- [9] M. Grimmer, M. Eslamy, S. Glied *et al.*, "A comparison of parallel-and series elastic elements in an actuator for mimicking human ankle joint in walking and running," in *IEEE International Conference on Robotics and Automation*, 2012, pp. 2463–2470.

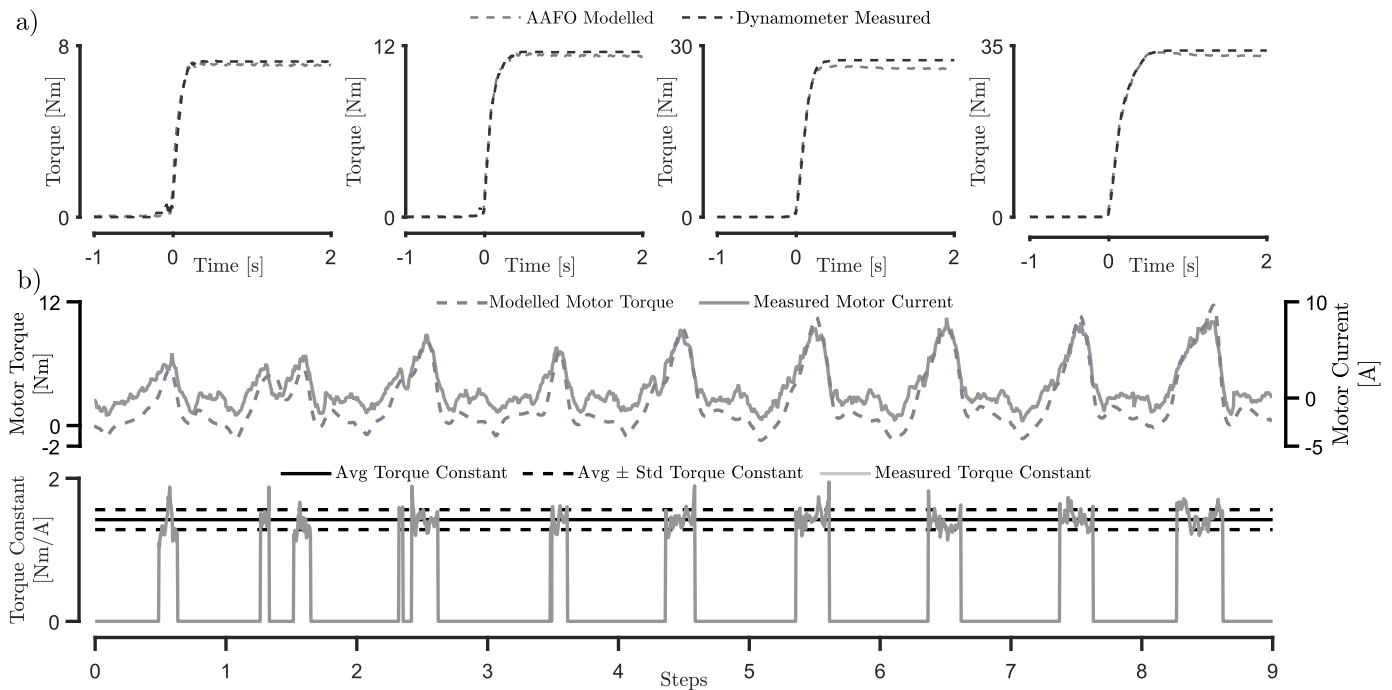


Fig. 7. a) AAFO static load dynamometer testing at various step inputs. The results compare the modelled ankle torque based on the actuator displacement (19)-(22) to a measured torque on a dynamometer. b) Human walking trial modelled motor torque, current, and inferred torque constant results.

- [10] J. Liu, N. A. A. Osman, M. A. Kouzbary *et al.*, "Optimization and comparison of typical elastic actuators in powered ankle-foot prosthesis," *International Journal of Control, Automation and Systems*, vol. 20, no. 1, pp. 232–242, 2022.
- [11] M. Moltedo, T. Bacek, K. Junius *et al.*, "Mechanical design of a lightweight compliant and adaptable active ankle foot orthosis," in *IEEE International Conference on Biomedical Robotics and Biomechatronics (BioRob)*, 2016, pp. 1224–1229.
- [12] A. M. Soliman, I. Hussain, M. I. Awad *et al.*, "Design and modeling of a variable stiffness barrel mechanism for ankle exoskeleton," in *International Design Engineering Technical Conferences and Computers and Information in Engineering Conference*. American Society of Mechanical Engineers Digital Collection, 2020.
- [13] Y. Ning, H. Huang, W. Xu *et al.*, "Design and implementation of a novel variable stiffness actuator with cam-based relocation mechanism," *Journal of Mechanisms and Robotics*, vol. 13, no. 2, p. 021009, 2021.
- [14] S. Sahoo, D. K. Pratihari, and S. Mukhopadhyay, "A novel energy efficient powered ankle prosthesis using four-bar controlled compliant actuator," *Proceedings of the Institution of Mechanical Engineers, Part C: Journal of Mechanical Engineering Science*, vol. 232, no. 24, pp. 4664–4675, 2018.
- [15] K. Deb, A. Pratap, S. Agarwal *et al.*, "A fast and elitist multiobjective genetic algorithm: NSGA-II," *IEEE transactions on evolutionary computation*, vol. 6, no. 2, pp. 182–197, 2002.